Evanescent gain for slow and stopped light in negative refractive index heterostructures

Edmund I. Kirby, Joachim M. Hamm, Tim W. Pickering, Kosmas L. Tsakmakidis, and Ortwin Hess[*]

Department of Physics, Imperial College London, London SW7 2AZ, United Kingdom

We theoretically and numerically analyze a five-layer "trapped rainbow" waveguide made of a passive negative refractive index (NRI) core layer and gain strips in the cladding. Analytic transfer-matrix calculations and full-wave time-domain simulations are deployed to calculate, both in the frequency and in the time domain, the losses or gain experienced by complex-wave-vector and complex-frequency modes. We find excellent agreement between five distinct sets of results, showing that the use of evanescent pumping (gain) can compensate the losses in the NRI slow- and stopped-light regimes.

PACS number(s): 78.67.Pt, 42.25.Bs, 78.20.Ci, 78.45.+h

The ability to stop and store optical pulses could usher in a range of fundamentally new and revolutionary applications,[1,2] but the challenges encountered in our efforts to stop light are formidable. This highly unusual state for an electromagnetic wave refers to the situation where the light wave completely stops despite the absence of any dielectric or other barriers in the directions where it could propagate. Unlike the confinement or trapping of light inside a dielectric cavity, where one cannot spatially separate optical bits of information, a stopped-light structure would allow for sequentially stopping and storing spatially separated optical bits, thereby potentially leading to all-optical memories.[1,2] Unfortunately, stopping of light cannot be obtained with static (nonswitchable) periodic structures, such as photonic crystals or coupled-resonator optical waveguides, owing to their extreme sensitivity to disorder, which invariably destroys the zero-group-velocity (ZGV) point(s).[2] With atomic electromagnetically induced transparency one coherently imprints the shape of an optical pulse into an electronic spin excitation, i.e., light is "stored" but not stopped because at the ZGV point all photons are converted into atomic spins and light is completely extinguished.[3]

A method that could allow for true stopping of light in solid-state structures and at ambient conditions was first suggested in 2007.[4] Instead of relying on periodic back reflections or on resonances, the deceleration and stopping of light was therein based on the use of negative bulk, disorder insensitive,[5] electromagnetic parameters in waveguide heterostructures. In the tapered setup[4] a given light frequency stops at a predefined point inside the waveguide. The physical space occupied by the stopping of different light frequencies depends on the angle of the adiabatic taper (e.g., see Ref. [6]). In the uniform configuration[7] an "optical bit" is stored at the point where the incident light beam evanescently hits the negative-index waveguide. Here, the physical space occupied by each individual bit and the density of the stored information are solely determined by the width/divergence of the incident light beam (e.g., a laser beam, the tip of a scanning microscope, etc).

A central task in this method of stopping and storing light is to study whether the losses associated with the use of negative refractive index (NRI) metamaterials can be overcome. Although a series of recent works[8] has shown that losses in active "fishnet" metamaterials can be compensated, the considered structures were very thin in the longitudinal direction, essentially being two dimensional and spatially dispersive. Furthermore, the dispersion relations and restrictions obeyed by light in fishnet metamaterials are completely different from those in trapped rainbow NRI waveguides. As a result, it is not clear until now whether in such waveguides losses can, even in principle, be overcome in a slow-/stopped-light regime where the effective refractive index experienced by light is negative—even when use is made of gain media.[9]

In this Rapid Communication, on the basis of analytical calculations and rigorous numerical simulations, we show how the incorporation of thin layers of a gain medium in a passive trapped rainbow heterostructure can compensate the losses while simultaneously preserving the negative effective refractive index of the guided slow or stopped light. The specific structure considered is illustrated in Fig. 1. It consists of a NRI core layer bounded symmetrically by two thin gain layers that evanescently feed the supported guided modes.[11] The whole structure is embedded in air.

When gain or losses are present in one or more of the layers of a heterostructure the supported guided modes become complex. Apart from the usual complex-wave-vector (real-frequency) solutions to the characteristic equation, one may then also retrieve complex-frequency (real-wave-vector) solutions.[12] For instance, it is well known from prism coupling to uniform metallic films that fixing the incident light frequency and sweeping the angle of incidence results in the excitation of complex-k surface-plasmon polaritons (SPPs) exhibiting back bending in the ω-k dispersion diagram. In contrast, keeping the incident angle constant and varying the frequency of the incident light gives rise to the excitation of complex-ω SPPs with distinct reflectivity dips and no back bending.[12] The imaginary part of a complex-ω solution relates to the temporal losses experienced by a light pulse.[12]

A numerical framework that is well suited for the study of these modes is the finite-difference time-domain (FDTD) method.[13] With this method one can accurately launch the desired negative phase velocity (backward) mode into the waveguide and directly investigate its temporal losses.[14] In our simulations we deploy a modified total-field/scattered-field formulation,[13] with the excitation plane oriented perpendicularly to the central axis of the heterostructure of Fig. 1, and the amplitudes of the H_z- and E_x-field components along the plane being set to match the transverse profile of the backward TM_2^b mode. The central frequency of the injected
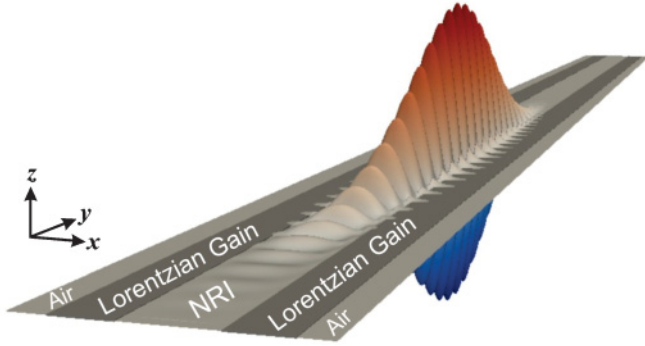
FIG. 1. (Color online) Illustration of the NRI slow-light heterostructure considered in the analyses. Also shown is a characteristic snapshot (from the FDTD simulations) of the propagation of the excited (dominant) slow-light mode. See also Ref. 10.

pulse is fixed to 400 THz ($\lambda_0 = 750$ nm), the side of the square FDTD cell has a length of $\Delta x = \lambda_0/200 = 3.75$ nm, and the Courant value is set to 0.7. The width of the core layer is $w_c = 0.35\lambda_0 = 262.5$ nm, while the width of the gain layers in the cladding is $w_g = 0.25\lambda_0 = 187.5$ nm whenever they are incorporated into the heterostructure. We model the passive NRI of the core layer using a broadband Drude response (see Ref. 15, Chap. 1.3)]: $n_D(\omega) = 1 - \omega_p^2/(\omega^2 + i\omega\Gamma_D)$, with $\omega_p = 2\pi \times 893.8 \times 10^{12}$ rad/s and $\Gamma_D = 0.27 \times 10^{12}\,\mathrm{s}^{-1}$. The frequency response of the permittivity of the gain layer obeys a Lorentzian dispersion: $\epsilon_L(\omega) = \epsilon_\infty + \Delta\epsilon\omega_L^2/(\omega_L^2 - i2\Gamma_L\omega - \omega^2)$, with $\epsilon_\infty = 1.001$, $\Delta\epsilon = -\ 0.0053$, $\omega_L = 2\pi \times 370 \times 10^{12}$ rad/s, and $\Gamma_L = 10^{14}\,\mathrm{s}^{-1}$, resulting in a line shape that is similar to that produced by, e.g., an electronic transition in a quantum dot.[16]

When the losses and gain are relatively small, as those used in the considered NRI heterostructure, the imaginary part of the complex-ω solution is proportional to the imaginary part of the complex-k solution by a factor that is close-to-equal to the group velocity.[17] Hence, in this case, one has an additional opportunity (see Fig. 4 later on) to check the accuracy of the obtained numerical results by examining whether such a proportionality is fulfilled. Following the standard theory of active optical waveguides,[18] we assume that the saturation intensity for the gain medium is sufficiently large, leading to a correspondingly large value of the critical gain-length product beyond which gain depletion owing to amplified spontaneous emission (ASE) can become significant.[19] Operation sufficiently below this limit implies that we are in the linear regime where no gain depletion occurs, and that the effect of ASE on the signal gain may be disregarded, in accordance with analogous studies of active optical structures.[18,20,21]

The mode-launching methodology described above allows for the clean excitation and study of individual modes along a uniform NRI heterostructure. However, it cannot be applied at exactly the light-stopping point because therein the injected light stays localized at the excitation plane. To study the loss compensation in that regime, we have developed a frequency-domain transfer-matrix method (TMM) capable of identifying both the complex-ω and complex-k modes of the multilayer NRI heterostructure. The method derives the dispersion equation and uses the argument principle method

to locate and isolate its zeros either on the complex-ω or the complex-k plane.[22] Suitable conformal mappings are deployed in both cases to unfold the four-sheeted Riemann surfaces associated with the characteristic equations. Upon isolation of a zero, the Newton-Raphson method is used to pinpoint and track its location on the complex plane. The technical details of the overall procedure will be presented elsewhere.

In our analyses we consider the following four cases: (I) neither loss in the NRI core layer ($\Gamma_D = 0$) nor gain in the cladding layers (the cladding is only air), (II) loss in the NRI core layer but no gain in the cladding, (III) both loss in the NRI region and gain in the cladding strips, and (IV) the NRI core layer is modeled as being lossless and gain is used in the two cladding layers.

In order to validate the causal dynamics of the injected pulse with the FDTD method we created an animation of its propagation along the considered heterostructure.[10] From there one may directly see that first, a single slow-light guided mode is excited and second, the mode experiences an effective refractive index n_{eff} with a negative real part, having antiparallel phase and group velocities.

Successive snapshots of the Gaussian pulse propagating down the NRI waveguide for cases I–IV are depicted in Fig. 2. We see that for case I (neither loss nor gain) the intensity of the guided pulse decays with distance [Fig. 2(a)]. This reduction is not a result of the pulse losing energy but arises entirely owing to group-velocity dispersion, which causes the guided slow pulse to broaden, thereby leading to a gradual decay in amplitude. Figure 3 (red line and downward triangles) confirms the fact that energy is conserved, as the absorption coefficient $\alpha = 2\omega\,\mathrm{Im}\{n_{eff}\}/c$ (spatial losses) is zero throughout the frequency spectrum of the pulse. The complex n_{eff} shown in Fig. 3 for all considered cases is extracted by recording the amplitude of the pulse at two fixed points along the central axis of the waveguide over time, and then dividing the Fourier transforms of the two time series.[13,14] When dissipative loss is introduced into the NRI core (case II) the amplitude of the pulse decreases even further compared to
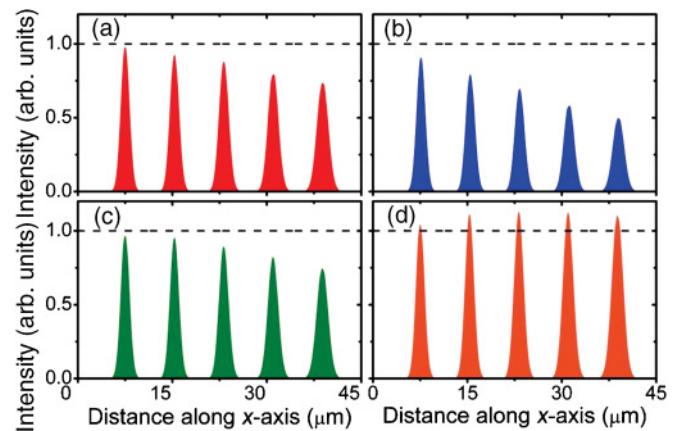
FIG. 2. (Color online) Snapshots of slow-light pulse propagation along the central axis of the considered waveguides for (a) case I (neither loss nor gain); (b) case II (loss but no gain); (c) case III (both, loss and gain); and (d) case IV (gain but no loss). In all cases propagation is from left to right.
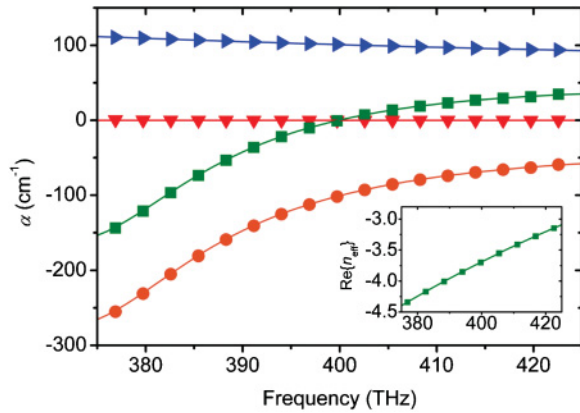
FIG. 3. (Color online) Comparison between FDTD (symbols) and TMM (lines) calculations of the absorption coefficient α (spatial losses) versus frequency for the TM_2^b mode in case I (red line, downward triangles), case II (blue line, right triangles), case III (green line, squares), and case IV (orange line, circles). The inset depicts the frequency dispersion of $Re\{n_{eff}\}$ in all four cases.

case I [Fig. 2(b)]. Figure 3 (blue line and right triangles) shows that now $Im\{n_{eff}\} > 0$ for all frequencies, as expected.

By introducing gain in the cladding layers (case III) we evanescently pump the pulse[11] and allow for the compensation of its propagation losses [compare Fig. 2(c) with Fig. 2(a)]. Indeed, Fig. 3 (green line and squares) shows that at approximately 400 THz (central frequency of the pulse) the imaginary part of the effective refractive index becomes zero, while for smaller frequencies $Im\{n_{eff}\}$ assumes negative values (amplification). Thus, in case III there is a continuous range of frequencies ($f < 400$ THz) where we simultaneously have $Re\{n_{eff}\} < 0$ (inset in Fig. 3) and $Im\{n_{eff}\} < 0$ (green line and squares for $f < 400$ THz in Fig. 3). We note that the optogeometric parameters of the heterostructure have been chosen such that a light pulse experiences almost the same frequency dispersion for all cases, with differences between the various $Re\{n_{eff}\}$ (cases I–IV) being indiscernible at the linear scale of the inset in Fig. 3. For all cases presented we find that the parameters retrieved from the FDTD simulations (symbols) are in excellent agreement with those calculated using the TMM (lines).

To further confirm that light amplification is, in principle, possible in the negative index slow-light regime we "switch off" the losses, while maintaining the gain in the cladding strips. Figure 2(d) shows that in this case (IV) the negative-phase-velocity slow pulse is amplified while propagating along the waveguide. In particular, it is seen that the pulse amplitude at around $x = 40$ μm exceeds its initial amplitude despite the fact that the pulse has been broadened due to group-velocity dispersion. This conclusion is further confirmed by finding that $Im\{n_{eff}\} < 0$ throughout the spectrum of the Gaussian pulse, as shown in Fig. 3 (orange line and circles).

Next, we examine how the spatial and temporal losses (or gain) experienced by both the central frequency of the pulse and the pulse as a whole vary with core thickness (Fig. 4). The complex-ω solutions can be calculated with the FDTD method by recording the spatial variation of the field amplitude along the central axis of the heterostructure at two different time points, and then dividing the spatial Fourier transforms of the
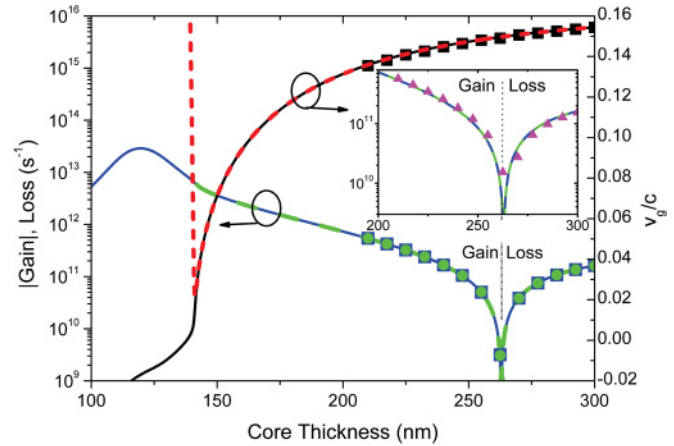
FIG. 4. (Color online) Comparison between FDTD (symbols) and TMM (lines) calculations of the temporal losses/gain and group velocity of the complex-ω and complex-k solutions with varying core thickness (case III). Shown are the group velocity (v_g) of the complex-ω solutions (black solid line, black squares), the group velocity of the complex-k solutions (red dashed line), the imaginary part of the complex-ω solutions (blue solid line, blue squares), and the imaginary part of the complex-k solutions multiplied by v_g (green dashed line, green circles). The inset shows the rate of energy loss (or gain) for the whole wave packet (purple triangles) with varying core thickness as calculated by the discrete Poynting's theorem within the FDTD method.

two longitudinal spatial profiles. The rate of energy change for the whole wave packet (total loss or gain) is calculated using the discrete Poynting's theorem integrated over a spatial region sufficiently wide to contain the pulse.

Figure 4 shows that for core thicknesses above 262 nm the central frequency of the pulse experiences loss. For smaller thicknesses, for which the amplitude of the field increases inside the gain region, we find that the gain supplied by the cladding strips overcompensates the loss induced by the core layer. At a core thickness of 262 nm the central frequency experiences neither gain nor loss, while the wave packet as a whole experiences gain (inset in Fig. 4). In all cases we have verified that $Re\{n_{eff}\} < 0$ (data not shown here).

Overall, we find excellent agreement and consistency between five distinct sets of results: the spatial losses/gain (multiplied by the group velocity[17]) for the central frequency as calculated by the FDTD (green circles) and the TMM (green dashed line), the temporal losses/gain for the central frequency as calculated by the FDTD (blue squares) and TMM (blue solid line), and the temporal losses of the *whole wave packet* as calculated by the FDTD method (purple triangles in the inset of Fig. 4). This fact provides further evidence that loss compensation is, in principle, possible in the slow-light NRI regime, including the light-stopping point at around 137 nm.

Finally, we note that for core thicknesses smaller than around 140 nm the group velocity of the complex-k mode characteristically differs from that of the complex-ω mode (red dashed and black solid lines in Fig. 4, respectively). As with the case of SPPs in plasmonic films,[12] the group velocity of the complex-k solutions exhibits a "back bending," never becoming zero, while that associated with the complex-ω solutions may reduce to zero or become negative (antiparallel

phase and group velocites), even in the presence of excessive gain (or losses).

In conclusion, by studying in the time and frequency domains the complex-ω and complex-k modes in NRI slow-light waveguides with gain in the cladding region, we have shown that it is possible to compensate the dissipative optical losses. This geometry allows for lossless or amplified slow/stopped light in the regime where the real part of the effective refractive index experienced by the guided modes remains negative. We believe that this work could aid the realization of lossless metamaterial waveguides to be used in a wealth of photonic and quantum optics applications.

---

[*] o.hess@imperial.ac.uk

[1] P. W. Milonni, *Fast Light, Slow Light and Left-Handed Light* (Taylor & Francis, New York, 2005).

[2] *Slow Light: Science and Applications*, edited by J. B. Khurgin and R. S. Tucker (Taylor & Francis, New York, 2009).

[3] M. D. Lukin and A. Imamoglu, Nature (London) **413**, 273 (2001).

[4] K. L. Tsakmakidis, A. Boardman, and O. Hess, Nature (London) **450**, 397 (2007).

[5] R. Singh, X. Lu, J. Gu, Z. Tian, and W. Zhang, J. Opt. **12**, 015101 (2010).

[6] V. N. Smolyaninova, I. I. Smolyaninov, A. V. Kildishev, and V. M. Shalaev, Appl. Phys. Lett. **96**, 211121 (2010).

[7] K. L. Tsakmakidis, E. I. Kirby, and O. Hess, Proc. SPIE **7612**, 76120U (2010); Q. Bai, J. Chen, N.-H. Shen, C. Cheng, and H.-T. Wang, Opt. Express **18**, 2106 (2010); Q. Gan, Z. Fu, Y. Ding, and F. Bartoli, Phys. Rev. Lett. **100**, 256803 (2008).

[8] S. Xiao, V. P. Drachev, A. V. Kildishev, X. Ni, U. K. Chettiar, H.-K. Yuan, and V. M. Shalaev, Nature (London) **466**, 735 (2010); S. Wuestner, A. Pusch, K. L. Tsakmakidis, J. M. Hamm, and C. Hess, Phys. Rev. Lett. **105**, 127401 (2010); A. Fang, T. Koschny, and C. M. Soukoulis, Phys. Rev. B **82**, 121102(R) (2010).

[9] A. Reza, M. M. Dignam, and S. Hughes, Nature (London) **455**, E10 (2008); K. L. Tsakmakidis, A. D. Boardman, and O. Hess, *ibid.* **455**, E11 (2008).

[10] See Supplemental Material at http://link.aps.org/supplemental/10.1103/PhysRevB.84.041103 for a QuickTime movie illustrating an example (case IV) of the propagation of the excited negative-phase-velocity slow-light mode along the waveguide heterostructure of Fig. 1. Similar dynamics (negative phase velocity) are seen for cases I–III.

[11] A. W. Fang, H. Park, O. Cohen, R. Jones, M. J. Paniccia, and J. E. Bowers, Opt. Express **14**, 9203 (2006).

[12] R. W. Alexander, G. S. Kovener, and R. J. Bell, Phys. Rev. Lett. **32**, 154 (1974); R. W. Gammon and E. D. Palik, J. Opt. Soc. Am. **64**, 350 (1974); G. S. Kovener, J. R. W. Alexander, and R. J. Bell, Phys. Rev. B **14**, 1458 (1976); A. Archambault, T. V. Teperik, F. Marquier, and J. J. Greffet, *ibid.* **79**, 195414 (2009).

[13] *Computational Electrodynamics: The Finite-Difference Time-Domain Method*, 3rd ed., edited by A. Taflove and S. C. Hagness (Artech House, Norwood, MA, 2005).

[14] E. I. Kirby, J. M. Hamm, K. L. Tsakmakidis, and O. Hess, J. Opt. A: Pure Appl. Opt. **11**, 114027 (2009).

[15] *Metamaterials: Physics and Engineering Explorations*, edited by N. Engheta and R. W. Ziolkowski (Wiley IEEE Press, New Jersey, 2006).

[16] A. A. Govyadinov, V. A. Podolskiy, and M. A. Noginov, Appl. Phys. Lett. **91**, 191103 (2007).

[17] K. C. Huang, E. Lidorikis, X. Jiang, J. D. Joannopoulos, K. A. Nelson, P. Bienstman, and S. Fan, Phys. Rev. B **69**, 195111 (2004).

[18] H. C. Casey and M. B. Panish, *Heterostructure Lasers Part A: Fundamental Principles* (Academic, New York, 1978).

[19] P. W. Milonni and J. H. Eberly, *Lasers* (Wiley, New York, 1988).

[20] T. Jiang and Y. Feng, Opt. Lett. **34**, 3869 (2009); W. T. Lu, Y. J. Huang, B. D. F. Casse, R. K. Banyal, and S. Sridhar, Appl. Phys. Lett. **96**, 211112 (2010)

[21] N. Zheludev, S. Prosvirnin, N. Papasimakis, and V. Fedotov, Nat. Photonics **2**, 351 (2008).

[22] M.-S. Kwon and S.-Y. Shin, Opt. Commun. **233**, 119 (2004).